YMTHE, Volume *26*

Supplemental Information

In Vivo Selection of a Computationally Designed SCHEMA AAV Library Yields a Novel Variant for Infection of Adult Neural Stem Cells in the SVZ

David S. Ojala, Sabrina Sun, Jorge L. Santiago-Ortiz, Mikhail G. Shapiro, Philip A. Romero, and David V. Schaffer

SUPPLEMENTARY INFORMATION

Figure S1. Inversion of *cap* in recombinase deficient Sure2 *E. coli* was detectable by PCR but not restriction digest. Lox66 and lox71 sites flanking stuffer sequences of 83, 95, 110, or 125 base pairs were cloned between the *Xho*I and *Kpn*I sites of pSub2RepKO. Constructs were transformed into competent *E. coli* expressing Cre recombinase (StrataClone) or recombinase-deficient Sure2 (Agilent), plasmid DNA was purified, and PCR was performed to amplify inverted genomes. Inverted amplicons were observed for both bacterial strains, indicating low levels of recombination that could lead to false positives during selections. Recombination was not detected by restriction digest.

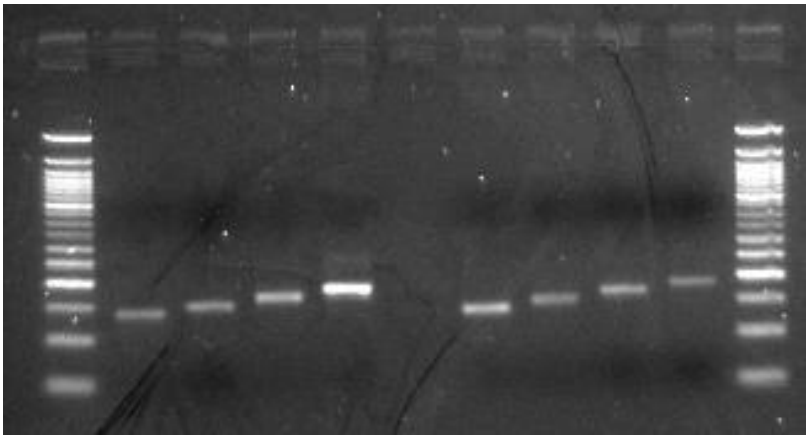

Lane	1	2	3	4	5	6	7	8	9	10	11
Sample	50 bp DNA Ladder (NEB N3236L)	83 bp stuffer, Cre +	95 bp stuffer, Cre +	110 bp stuffer, Cre +	125 bp stuffer, Cre +		83 bp stuffer, recombinase deficient Sure2	95 bp stuffer, recombinase deficient Sure2	110 bp stuffer, recombinase deficient Sure2	125 bp stuffer, recombinase deficient Sure2	50 bp DNA Ladder (NEB N3236L)

Figure S2. SCH9 and SCH2 *cap* amino acid sequences.

SCH9:

MAADGYLPDWLEDNLSEGIREWWDLKPGAPKPKANQQKQDDGRGLVLPGYKYLGPFNGL
DKGEPVNAADAAALEHDKAYDQQLKAGDNPYLRYNHADAEFQERLQEDTSFGGNLGRAV
FQAKKRVLEPLGLVEEAAKTAPGKKRPVEQSPQEPDSSAGIGKSGAQPAKKRLNFGQTGDT
ESVPDPQPIGEPPAAPSGVGSLTMASGGGAPVADNNEGADGVGSSSGNWHCDSQWLGDRVI
TTSTRTWALPTYNNHLYKQISNSTSGGSSNDNAYFGYSTPWGYFDFNRFHCHFSPRDWQRLI
NNNWGFRPKRLSFKLFNIQVKEVTQNEGTKTIANNLTSTIQVFTDSDYQLPYVLGSAHEGCL
PPFPADVFMIPQYGYLTLNDGSQAVGRSSFYCLEYFPSQMLRTGNNFQFSYEFENVPFHSSY
AHSQSLDRLMNPLIDQYLYYLSKTINGSGQNQQTLKFSVAGPSNMAVQGRNWLPGPCYRQ
QRVSKTSADNNNSEYSWTGATKYHLNGRDSLVNPGPAMASHKDDEEKFFPQSGVLIFGKQ
GSEKTNVDIEKVMITDEEEIRTTNPVATEQYGSVSTNLQRGNRQAATADVNTQGVLPGMVW
QDRDVYLQGPIWAKIPHTDGNFHPSPLMGGFGMKHPPPQILIKNTPVPADPPTAFNKDKLNS
FITQYSTGQVSVEIEWELQKENSKRWNPEIQYTSNYYKSNNVEFAVNTEGVYSEPRPIGTRY
LTRNL

SCH2:

MAADGYLPDWLEDNLSEGIREWWDLKPGAPKPKANQQKQDDGRGLVLPGYKYLGPFNGL
DKGEPVNAADAAALEHDKAYDQQLKAGDNPYLRYNHADAEFQERLQEDTSFGGNLGRAV
FQAKKRVLEPLGLVEEAAKTAPGKKRPVEQSPQEPDSSAGIGKSGAQPAKKRLNFGQTGDT
ESVPDPQPIGEPPAAPSGVGSLTMASGGGAPVADNNEGADGVGSSSGNWHCDSQWLGDRVI
TTSTRTWALPTYNNHLYKQISNSTSGGSSNDNAYFGYSTPWGYFDFNRFHCHFSPRDWQRLI
NNNWGFRPKRLSFKLFNIQVKEVTQNEGTKTIANNLTSTIQVFTDSDYQLPYVLGSAHEGCL
PPFPADVFMIPQYGYLTLNDGSQAVGRSSFYCLEYFPSQMLRTGNNFQFSYTFEDVPFHSSY
AHSQSLDRLMNPLIDQYLYYLSRTNTPSGTTTQSRLQFSQAGASDIRDQSRNWLPGPCYRQQ
RVSKTSADNNNSEYSWTGATKYHLNGRDSLVNPGPAMASHKDDEEKFFPQSGVLIFGKQGS
EKTNVDIEKVMITDEEEIRTTNPVATEQYGSVSTNLQRGNRQAATADVNTQGVLPGMVWQ
DRDVYLQGPIWAKIPHTDGNFHPSPLMGGFGMKHPPPQILIKNTPVPADPPTAFNKDKLNSFI
TQYSTGQVSVEIEWELQKENSKRWNPEIQYTSNYYKSNNVEFAVNTEGVYSEPRPIGTRYLT
RNL

Figure S3. Alignment of the SCH9 and SCH2 AAV *cap* amino acid sequences with the parent AAV serotypes. Capsid sequences were aligned using the Geneious program (Biomatters). Colored amino acids represent differences relative to the reference SCH9 *cap* sequence. Amino acids involved in heparin or galactose binding are annotated in green and blue, respectively, above the SCH9 sequence.

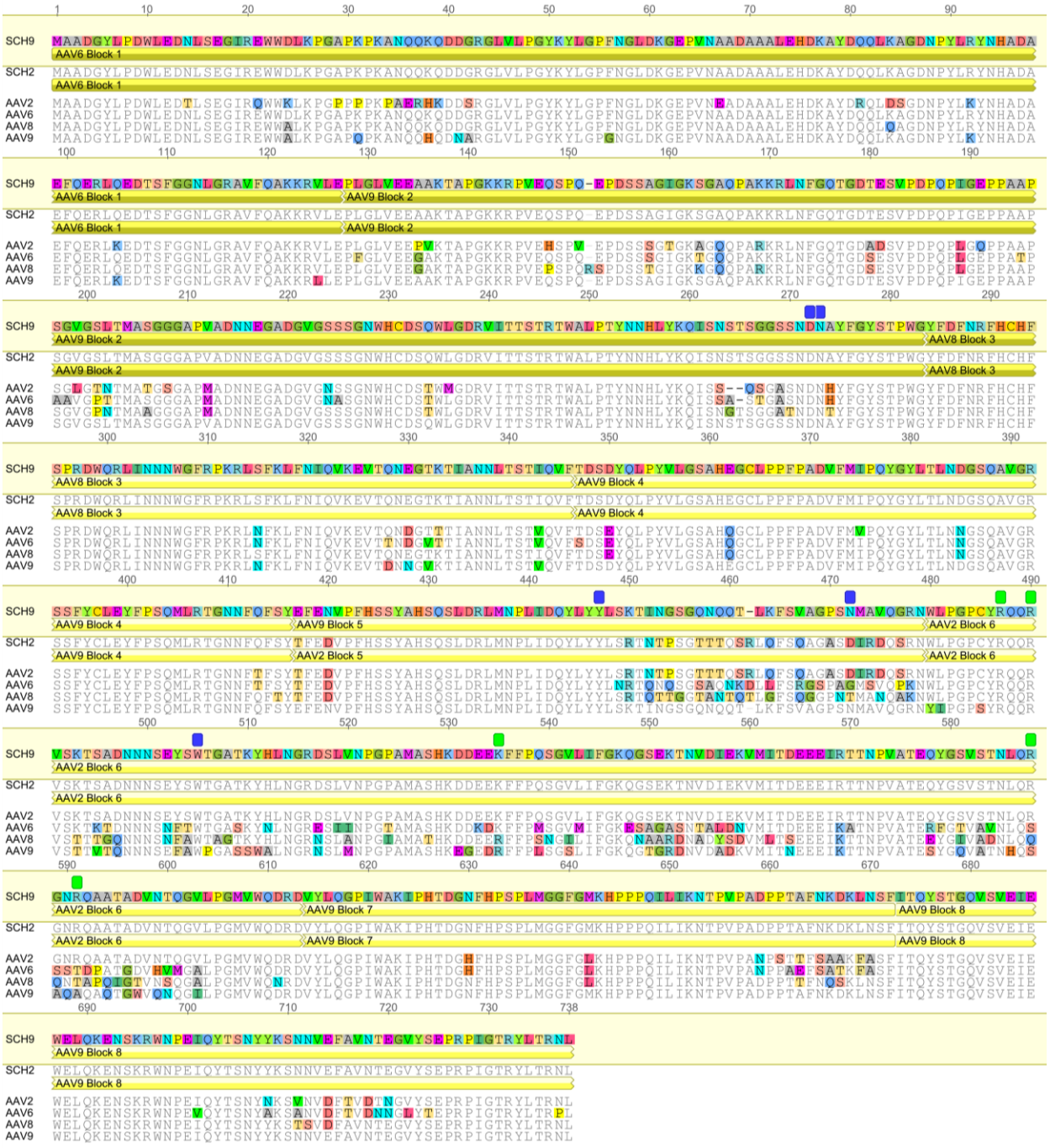

Figure S4. Viral genomic yield of recombinant self-complementary AAV vectors. Data are normalized to the cell culture surface area and are presented as mean ± SD, n=3.

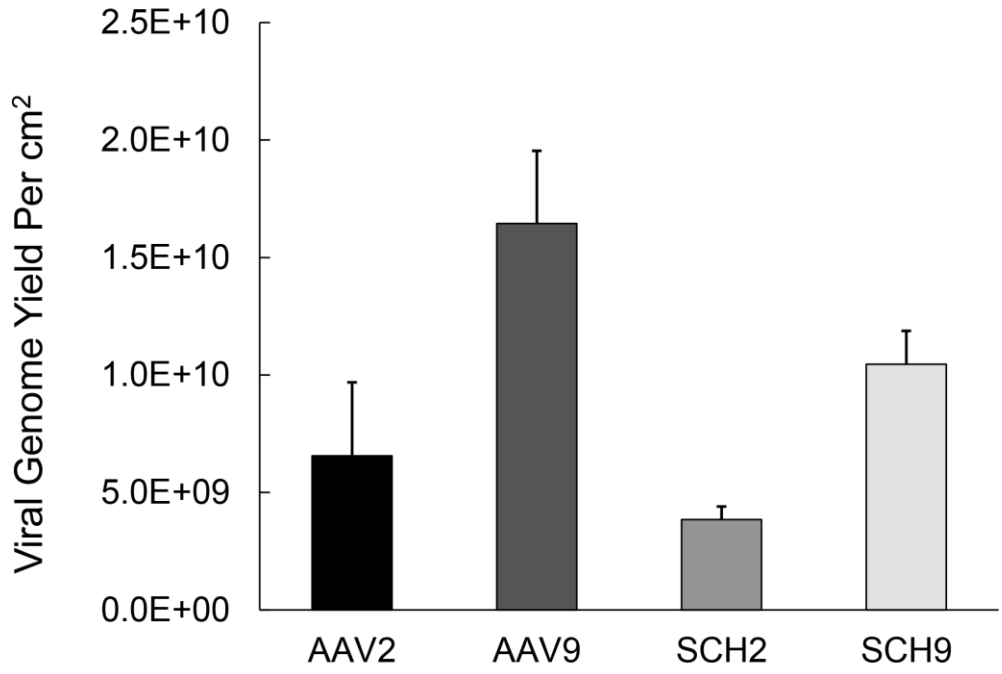

Figure S5. GFP expression in the cerebellum three weeks after unilateral injection of recombinant AAV1 or SCH9 into the deep cerebellar nuclei. Coronal sections were stained for GFP (green) and the Purkinje cell marker calbindin (purple). Scale bars indicate 500 µm.

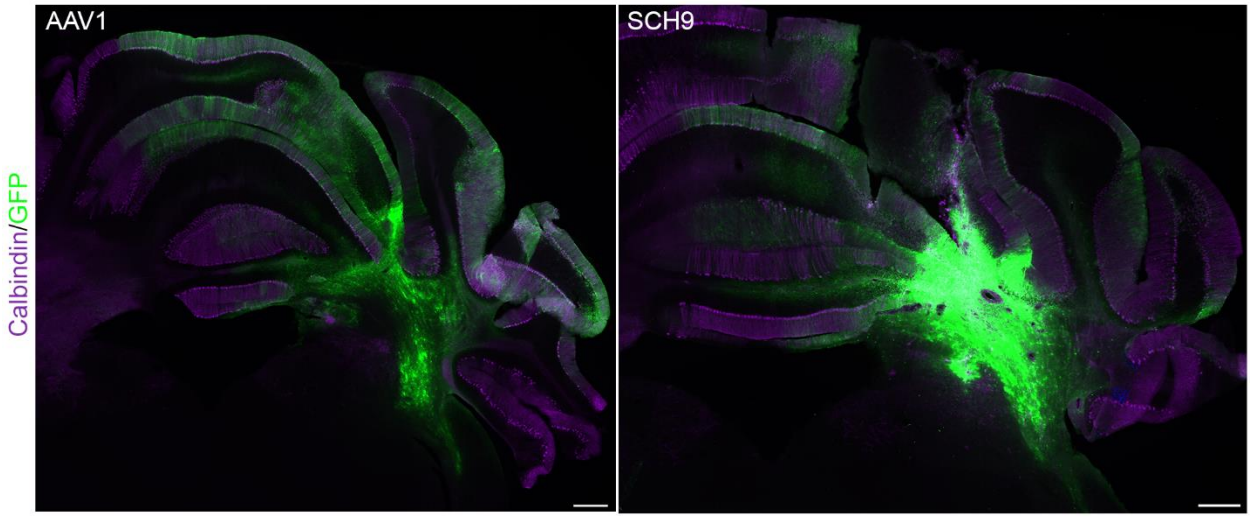

Figure S6. Confocal analysis of GFP expression in the striatum three weeks after injection of recombinant AAV1 or SCH9. Coronal sections were stained for GFP (green), the astrocyte marker GFAP (), and the neuronal marker NeuN (red). Scale bars indicate 25 µm. Image analysis was performed by counting colocalized cells in ImageJ (over 225 cells counted per mouse).

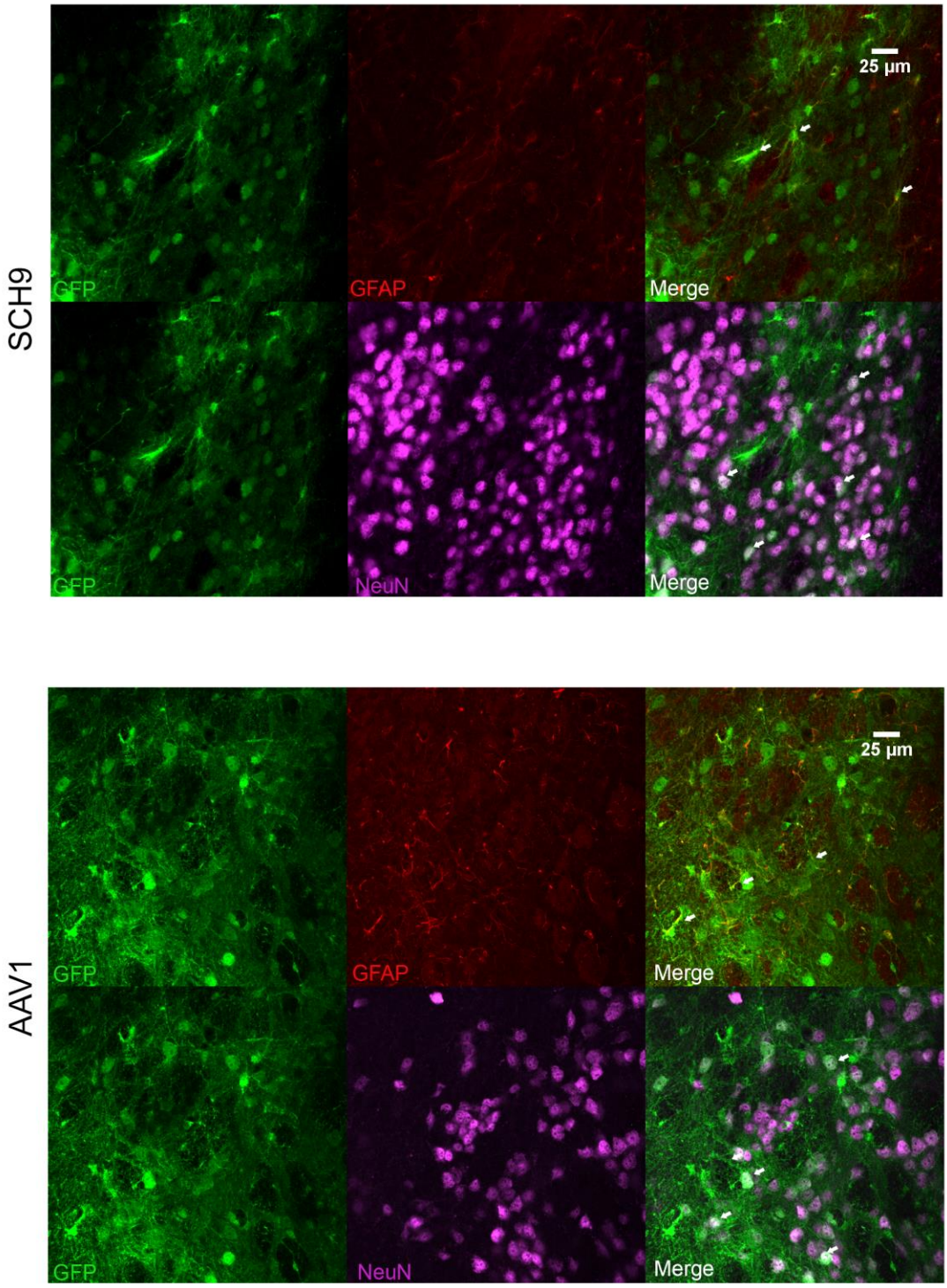

Figure S7. SCH2 and SCH9 are unable to infect a HeLa AAVR knockout cell line. The infectivity of SCH2 and SCH9 was compared with AAV2, a control that is known to utilize AAVR. All three variants efficiently transduce wild type HeLa cells, but not the AAVR knockout line. Data are presented as mean ± SEM, n = 6. *, statistical difference of $P < 0.005$ by two-tailed Student's t-test.

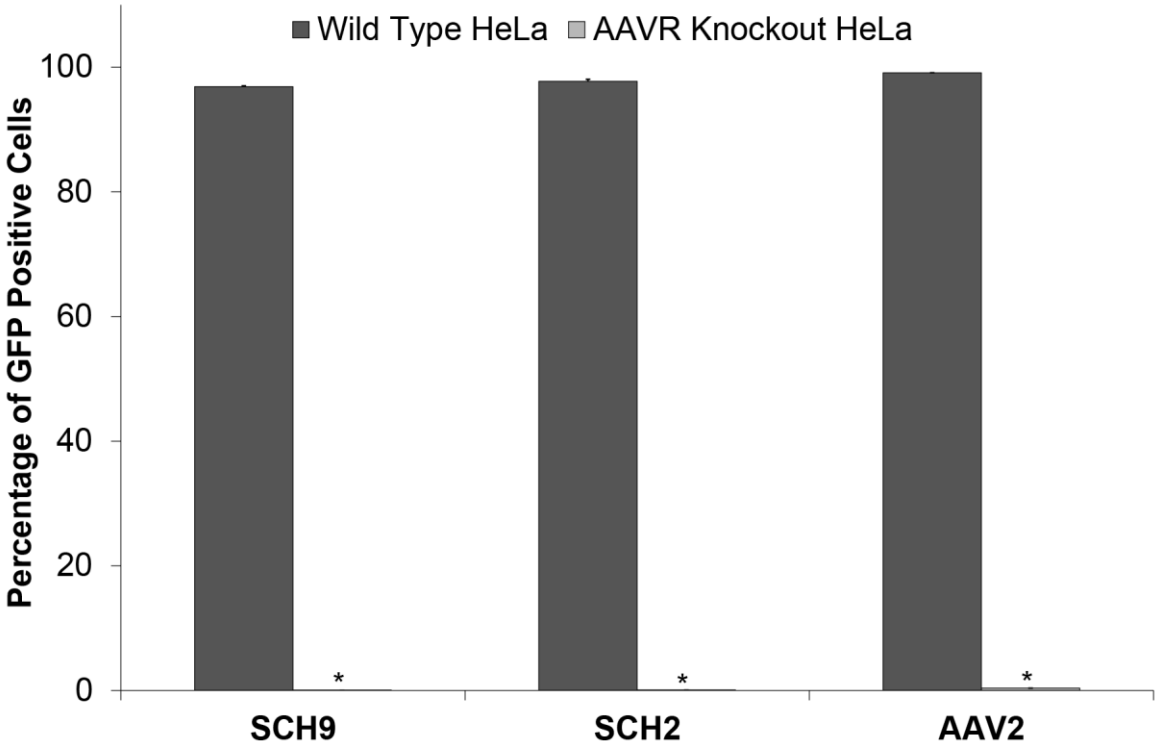

Table S1. Neutralizing IVIG titers of SCH9 and the parent serotypes from which it is derived. The neutralizing titers represent the first IVIG concentration at which 50% or greater reduction in GFP expression was observed.

Variant	Neutralizing IVIG Concentration (mg/mL)	SCH9 Fold Improvement
SCH9	0.20	N/A
AAV2	0.10	2
AAV6	0.10	2
AAV8	0.10	2
AAV9	0.02	10

Table S2. Primer sequences used in this study to design constructs and amplify the AAV *cap* gene.

Primer name	**Primer sequence (5'-3')**
QC_pBluescript_Fwd	GCTGCAATGATACCGCGAAACCCACGCTC
QC_pBluescript_Rev	GAGCGTGGGTTTCGCGGTATCATTGCAGC
QC_AAV4_Fwd	GCTCCTGGAAAGAAGAGGCCGTTGATTGAATCCCC
QC_AAV4_Rev	GGGGATTCAATCAACGGCCTCTTCTTTCCAGGAGC
QC_AAV5_Fwd	GACCCGGAAACGGACTCGATCGAGGAG
QC_AAV5_Rev	CTCCTCGATCGAGTCCGTTTCCGGGTC
QC_AAV6_Fwd	GTTTAGCCGGGGCTCTCCAGCTGGC
QC_AAV6_Rev	GCCAGCTGGAGAGCCCCGGCTAAAC
QC_AAV8_Fwd	CTCCTGGAAAGAAGAGGCCGGTAGAGCCATCAC
QC_AAV8_Rev	GTGATGGCTCTACCGGCCTCTTCTTTCCAGGAG
BglIIFwd	CAAGCGGCCGCGTAAGCTTAGATCTCTGACGTCGATGGCTG CG
BglIIRev	CGCAGCCATCGACGTCAGAGATCTAAGCTTACGCGGCCGCT TG
Lox66Fwd	GATCTATAACTTCGTATAGCATACATTATACGAACGGTACG
Lox66Rev	CGTACCGTTCGTATAATGTATGCTATACGAAGTTATTTCGA
XhoIFwd	CCGCTTGTTAATCAATAAACCGTTTAATTCGTTTCAGTTGAC TCGAGGTCTCTGCGTATTTCTTTCT
XhoIRev	AGAAAGAAATACGCAGAGACCTCGAGTCAACTGAAACGAA TTAAACGGTTTATTGATTAACAAGCGG
KpnIFwd	CGTAGATAAGTAGCATGGCGGGTTAATCAGGTACCACAAG GAACCCCTAG
KpnIRev	CTAGGGGTTCCTTGTGGTACCTGATTAACCCGCCATGCTACT TATCTACG
SOELox71Fwd	GTCAGCCTCGAGATAACTTCGTATAATGTATGCTATACGAA CGGTACTGTGGTCGTCATTGGCAACTACACCTGTTCG
SOELox71Rev	CGTCACGGTACCTGTGGAATTGTGAGCGCTCACAATTCCAC AGCTAGCCTATTTACCGATACCACACGAACAGGTGTAGTTG CCAATGACG
Lox71Fwd	GTCAGCCTCGAGATAACTTCG
Lox71Rev	CGTCACGGTACCTGTGG
Cap_ISF	CATGGAAACTAGATAAGAAAGA
Cap_NSF	GGTACGAAGCTTCGATCAACTACGCAG
Cap_R	AGCTAGCCTATTTACCGATAC
Internal_Cap_ISF	AAGTTCAACTGAAACGAATTA
Internal_Cap_R	CACACGAACAGGTGTAGTT

Table S3. Primer sequences designed in j5 to amplify each sequence block for combinatorial golden gate assembly of the SCHEMA AAV library.

Primer name	Primer sequence (5'-3')
DO_02_(Vector_Backbone)_forward	CACACCAGGTCTCATTGCGCGCTTGGCGTAATCATGG
DO_03_(Vector_Backbone)_reverse	CACACCAGGTCTCATTATAGTGAGTCGTATTACGCGC
DO_04_(AAV2_b1)_forward	CACACCAGGTCTCAATAAGGCGAATTGGGTACCG
DO_05_(AAV2_b1)_reverse	CACACCAGGTCTCAGTTCAAGAACCCTCTTTTTCGC
DO_06_(AAV2_b2)_forward	CACACCAGGTCTCAGAACCTCTGGGCCTGGTTGAG
DO_07_(AAV2_b2)_reverse	CACACCAGGTCTCAACCCCCAAGGGGTGCTGTAG
DO_08_(AAV2_b3)_forward	CACACCAGGTCTCAGGGTATTTTGACTTCAACAGATTCCACTGC
DO_09_(AAV2_b3)_reverse	CACACCAGGTCTCAAAAGACCTGAACCGTGCTGG
DO_10_(AAV2_b4)_forward	CACACCAGGTCTCACTTTACTGACTCGGAGTACCAGC
DO_11_(AAV2_b4)_reverse	CACACCAGGTCTCAGTAGCTGAAGGTAAAGTTGTTTCC
DO_12_(AAV2_b5)_forward	CACACCAGGTCTCACTACACTTTTGAGGACGTTCC
DO_13_(AAV2_b5)_reverse	CACACCAGGTCTCAAGTTCCTAGACTGGTCCCGAATG
DO_14_(AAV2_b6)_forward	CACACCAGGTCTCAAACTGGCTTCCTGGACCCTG
DO_15_(AAV2_b6)_reverse	CACACCAGGTCTCAGTCTCTGTCCTGCCAGACCATG
DO_16_(AAV2_b7)_forward	CACACCAGGTCTCAAGACGTGTACCTTCAGGGGC
DO_17_(AAV2_b7)_reverse	CACACCAGGTCTCAATGAAGGAAGCAAACTTTGCCG
DO_18_(AAV2_b8)_forward	CACACCAGGTCTCATCATCACACAGTACTCCACGG
DO_19_(AAV2_b8)_reverse	CACACCAGGTCTCAGCAAGCGCGCAATTAACCCTC
DO_20_(AAV4_b1)_reverse	CACACCAGGTCTCAGTTCAAGAACCCTCTTTTTGGC
DO_21_(AAV4_b2)_forward	CACACCAGGTCTCAGAACCTCTTGGTCTGGTTGAG
DO_22_(AAV4_b2)_reverse	CACACCAGGTCTCAACCCCCAGGGGGTGGAGAAT
DO_23_(AAV4_b3)_forward	CACACCAGGTCTCAGGGTATTTTGACTTCAACCGCTTCC
DO_24_(AAV4_b3)_reverse	CACACCAGGTCTCAAAAGATCTGAACCGTGCTGG
DO_25_(AAV4_b4)_forward	CACACCAGGTCTCACTTTGCGGACTCGTCGTACG
DO_26_(AAV4_b4)_reverse	CACACCAGGTCTCAGTAGGTAATTTCAAAGTTGTTGCC
DO_27_(AAV4_b5)_forward	CACACCAGGTCTCACTACAGTTTTGAGAAGGTGCCT
DO_28_(AAV4_b5)_reverse	CACACCAGGTCTCAAGTTCTTTTTAAAGTTGGAAAAGTTGGT
DO_29_(AAV4_b6)_forward	CACACCAGGTCTCAAACTGGCTGCCCGGGCCTTC
DO_30_(AAV4_b6)_reverse	CACACCAGGTCTCAGTCTCTGTTTTGCCAGACCATTC
DO_31_(AAV4_b7)_forward	CACACCAGGTCTCAAGACATTTACTACCAGGGTCCC
DO_32_(AAV4_b7)_reverse	CACACCAGGTCTCAATGAAGGAGTTTACCGGAGTAGAG
DO_33_(AAV4_b8)_forward	CACACCAGGTCTCATCATTACTCAGTACAGCACTGGC
DO_34_(AAV4_b8)_reverse	CACACCAGGTCTCAGCAAGCGCGCAATTAACCCTCACTAAAGG
DO_35_(AAV5_b1)_reverse	CACACCAGGTCTCAGTTCGAGAACCCTTTTCTTGGC
DO_36_(AAV5_b2)_forward	CACACCAGGTCTCAGAACCTTTTGGCCTGGTTGAA
DO_37_(AAV5_b2)_reverse	CACACCAGGTCTCAACCCCCAGGGGGTGCTGTAT
DO_38_(AAV5_b3)_forward	CACACCAGGTCTCAGGGTATTTTGACTTTAACCGCTTCC
DO_39_(AAV5_b3)_reverse	CACACCAGGTCTCAAAAGACTTGGACGGTGGAGG
DO_40_(AAV5_b4)_forward	CACACCAGGTCTCACTTTACGGACGACGACTACC
DO_41_(AAV5_b4)_reverse	CACACCAGGTCTCAGTAGGTAAACTCAAAGTTGTTGCC
DO_42_(AAV5_b5)_forward	CACACCAGGTCTCACTACAACTTTGAGGAGGTGCC
DO_43_(AAV5_b5)_reverse	CACACCAGGTCTCAAGTTTTTGTAGGTGTTGGCGTATCTCC
DO_44_(AAV5_b6)_forward	CACACCAGGTCTCAAACTGGTTCCCGGGGCCCAT
DO_45_(AAV5_b6)_reverse	CACACCAGGTCTCAGTCTCTCTCCATCCACACGC
DO_46_(AAV5_b7)_forward	CACACCAGGTCTCAAGACGTGTACCTCCAAGGACC
DO_47_(AAV5_b7)_reverse	CACACCAGGTCTCAATGAAGCTGCTGACGGGCAC
DO_48_(AAV5_b8)_forward	CACACCAGGTCTCATCATCACCCAGTACAGCACC
DO_49_(AAV6_b1)_reverse	CACACCAGGTCTCAGTTCGAGAACCCTCTTCTTGG
DO_50_(AAV6_b2)_forward	CACACCAGGTCTCAGAACCTTTTGGTCTGGTTGAGG
DO_51_(AAV6_b2)_reverse	CACACCAGGTCTCAACCCCCAGGGGGTGCTGTAGC
DO_52_(AAV6_b3)_forward	CACACCAGGTCTCAGGGTATTTTGATTTCAACAGATTCCACTGC
DO_53_(AAV6_b3)_reverse	CACACCAGGTCTCAAAAGACTTGAACCGTGCTGG
DO_54_(AAV6_b4)_forward	CACACCAGGTCTCACTTTTCGGACTCGGAGTACC
DO_55_(AAV6_b4)_reverse	CACACCAGGTCTCAGTAGCTGAAGGTAAAGTTATTGCC
DO_56_(AAV6_b5)_forward	CACACCAGGTCTCACTACACCTTCGAGGACGTGC
DO_57_(AAV6_b5)_reverse	CACACCAGGTCTCAAGTTTTTGGGCTGAACAGACATGC
DO_58_(AAV6_b6)_forward	CACACCAGGTCTCAAACTGGCTACCTGGACCCTG
DO_59_(AAV6_b6)_reverse	CACACCAGGTCTCAGTCTCTGTCTTGCCACACCATTC
DO_60_(AAV6_b7)_forward	CACACCAGGTCTCAAGACGTATACCTGCAGGGTCC
DO_61_(AAV6_b7)_reverse	CACACCAGGTCTCAATGAATGAAGCAAACTTTGTAGCC
DO_62_(AAV6_b8)_forward	CACACCAGGTCTCATCATCACCCAGTATTCCACAGG
DO_63_(AAV8_b1)_reverse	CACACCAGGTCTCAGTTCGAGAACCCGCTTCTTGG
DO_64_(AAV8_b2)_forward	CACACCAGGTCTCAGAACCTCTCGGTCTGGTTGAG
DO_65_(AAV8_b2)_reverse	CACACCAGGTCTCAACCCCCAGGGGGTGCTGTAG
DO_66_(AAV8_b3)_forward	CACACCAGGTCTCAGGGTATTTTGACTTTAACAGATTCCACTGC
DO_67_(AAV8_b3)_reverse	CACACCAGGTCTCAAAAGACCTGGATGGTGCTGG
DO_68_(AAV8_b4)_forward	CACACCAGGTCTCACTTTACGGACTCGGAGTACC
DO_69_(AAV8_b4)_reverse	CACACCAGGTCTCAGTAGGTAAACTGGAAGTTGTTGC
DO_70_(AAV8_b5)_reverse	CACACCAGGTCTCAAGTTCTTTGCCTGATTGGCC
DO_71_(AAV8_b6)_forward	CACACCAGGTCTCAAACTGGCTGCCAGGACCCTG
DO_72_(AAV8_b6)_reverse	CACACCAGGTCTCAGTCTCGGTTCTGCCAGACCATAC
DO_73_(AAV8_b7)_forward	CACACCAGGTCTCAAGACGTGTACCTGCAGGGTCC
DO_74_(AAV8_b7)_reverse	CACACCAGGTCTCAATGAAAGAGTTCAGCTTTGACTGG
DO_75_(AAV8_b8)_forward	CACACCAGGTCTCATCATCACGCAATACAGCACCG
DO_76_(AAV9_b1)_reverse	CACACCAGGTCTCAGTTCAAGAAGCCTCTTTTTGGC
DO_77_(AAV9_b2)_forward	CACACCAGGTCTCAGAACCTCTTGGTCTGGTTGAGG
DO_78_(AAV9_b3)_reverse	CACACCAGGTCTCAAAAGACCTGGACCGTGCTGG
DO_79_(AAV9_b4)_forward	CACACCAGGTCTCACTTTACGGACTCAGACTATCAGC
DO_80_(AAV9_b4)_reverse	CACACCAGGTCTCAGTAGCTGAACTGGAAGTTGTTACC
DO_81_(AAV9_b5)_forward	CACACCAGGTCTCACTACGAGTTTGAGAACGTACC
DO_82_(AAV9_b5)_reverse	CACACCAGGTCTCAAGTTTCTTCCCTGGACAGCC
DO_83_(AAV9_b6)_forward	CACACCAGGTCTCAAACTACATACCTGGACCCAGC
DO_84_(AAV9_b6)_reverse	CACACCAGGTCTCAGTCTCTGTCCTGCCAAACCATACC
DO_85_(AAV9_b7)_forward	CACACCAGGTCTCAAGACGTGTACCTGCAAGGAC
DO_86_(AAV9_b7)_reverse	CACACCAGGTCTCAATGAAAGAGTTCAGCTTGTCCTTG
DO_87_(AAV9_b8)_forward	CACACCAGGTCTCATCATCACCCAGTATTCTACTGGC

Table S4. PCR reactions for combinatorial golden gate cloning of the SCHEMA AAV library.

Block ID Number	Primary Template	Forward Primer	Reverse Primer	Amplicon length (bp)
0	pBluescript SK +	DO_02_(Vector_Backbone)_forward	DO_03_(Vector_Backbone)_reverse	2843
1	AAV2	DO_04_(AAV2_b1)_forward	DO_05_(AAV2_b1)_reverse	784
2	AAV2	DO_06_(AAV2_b2)_forward	DO_07_(AAV2_b2)_reverse	491
3	AAV2	DO_08_(AAV2_b3)_forward	DO_09_(AAV2_b3)_reverse	220
4	AAV2	DO_10_(AAV2_b4)_forward	DO_11_(AAV2_b4)_reverse	242
5	AAV2	DO_12_(AAV2_b5)_forward	DO_13_(AAV2_b5)_reverse	222
6	AAV2	DO_14_(AAV2_b6)_forward	DO_15_(AAV2_b6)_reverse	433
7	AAV2	DO_16_(AAV2_b7)_forward	DO_17_(AAV2_b7)_reverse	211
8	AAV2	DO_18_(AAV2_b8)_forward	DO_19_(AAV2_b8)_reverse	298
9	AAV4	DO_04_(AAV2_b1)_forward	DO_20_(AAV4_b1)_reverse	784
10	AAV4	DO_21_(AAV4_b2)_forward	DO_22_(AAV4_b2)_reverse	467
11	AAV4	DO_23_(AAV4_b3)_forward	DO_24_(AAV4_b3)_reverse	220
12	AAV4	DO_25_(AAV4_b4)_forward	DO_26_(AAV4_b4)_reverse	251
13	AAV4	DO_27_(AAV4_b5)_forward	DO_28_(AAV4_b5)_reverse	225
14	AAV4	DO_29_(AAV4_b6)_forward	DO_30_(AAV4_b6)_reverse	445
15	AAV4	DO_31_(AAV4_b7)_forward	DO_32_(AAV4_b7)_reverse	211
16	AAV4	DO_33_(AAV4_b8)_forward	DO_34_(AAV4_b8)_reverse	298
17	AAV5	DO_04_(AAV2_b1)_forward	DO_35_(AAV5_b1)_reverse	787
18	AAV5	DO_36_(AAV5_b2)_forward	DO_37_(AAV5_b2)_reverse	467
19	AAV5	DO_38_(AAV5_b3)_forward	DO_39_(AAV5_b3)_reverse	220
20	AAV5	DO_40_(AAV5_b4)_forward	DO_41_(AAV5_b4)_reverse	248
21	AAV5	DO_42_(AAV5_b5)_forward	DO_43_(AAV5_b5)_reverse	204
22	AAV5	DO_44_(AAV5_b6)_forward	DO_45_(AAV5_b6)_reverse	442
23	AAV5	DO_46_(AAV5_b7)_forward	DO_47_(AAV5_b7)_reverse	208
24	AAV5	DO_48_(AAV5_b8)_forward	DO_19_(AAV2_b8)_reverse	298
25	AAV6	DO_04_(AAV2_b1)_forward	DO_49_(AAV6_b1)_reverse	784
26	AAV6	DO_50_(AAV6_b2)_forward	DO_51_(AAV6_b2)_reverse	494
27	AAV6	DO_52_(AAV6_b3)_forward	DO_53_(AAV6_b3)_reverse	220
28	AAV6	DO_54_(AAV6_b4)_forward	DO_55_(AAV6_b4)_reverse	242
29	AAV6	DO_56_(AAV6_b5)_forward	DO_57_(AAV6_b5)_reverse	222
30	AAV6	DO_58_(AAV6_b6)_forward	DO_59_(AAV6_b6)_reverse	433
31	AAV6	DO_60_(AAV6_b7)_forward	DO_61_(AAV6_b7)_reverse	211
32	AAV6	DO_62_(AAV6_b8)_forward	DO_19_(AAV2_b8)_reverse	298
33	AAV8	DO_04_(AAV2_b1)_forward	DO_63_(AAV8_b1)_reverse	784
34	AAV8	DO_64_(AAV8_b2)_forward	DO_65_(AAV8_b2)_reverse	500
35	AAV8	DO_66_(AAV8_b3)_forward	DO_67_(AAV8_b3)_reverse	220
36	AAV8	DO_68_(AAV8_b4)_forward	DO_69_(AAV8_b4)_reverse	242
37	AAV8	DO_56_(AAV6_b5)_forward	DO_70_(AAV8_b5)_reverse	222
38	AAV8	DO_71_(AAV8_b6)_forward	DO_72_(AAV8_b6)_reverse	433
39	AAV8	DO_73_(AAV8_b7)_forward	DO_74_(AAV8_b7)_reverse	211
40	AAV8	DO_75_(AAV8_b8)_forward	DO_19_(AAV2_b8)_reverse	298
41	AAV9	DO_04_(AAV2_b1)_forward	DO_76_(AAV9_b1)_reverse	787
42	AAV9	DO_77_(AAV9_b2)_forward	DO_51_(AAV6_b2)_reverse	491
43	AAV9	DO_08_(AAV2_b3)_forward	DO_78_(AAV9_b3)_reverse	220
44	AAV9	DO_79_(AAV9_b4)_forward	DO_80_(AAV9_b4)_reverse	242
45	AAV9	DO_81_(AAV9_b5)_forward	DO_82_(AAV9_b5)_reverse	219
46	AAV9	DO_83_(AAV9_b6)_forward	DO_84_(AAV9_b6)_reverse	433
47	AAV9	DO_85_(AAV9_b7)_forward	DO_86_(AAV9_b7)_reverse	211
48	AAV9	DO_87_(AAV9_b8)_forward	DO_34_(AAV4_b8)_reverse	298

Table S5. Unique block junctures specified during primer design to ensure efficient golden gate assembly.

Block Identity	Overhang with Previous Block	Overhang with Next Block
(Vector_Backbone)	TTGC	ATAA
(AAV2_b1)	ATAA	GAAC
(AAV2_b2)	GAAC	GGGT
(AAV2_b3)	GGGT	CTTT
(AAV2_b4)	CTTT	CTAC
(AAV2_b5)	CTAC	AACT
(AAV2_b6)	AACT	AGAC
(AAV2_b7)	AGAC	TCAT
(AAV2_b8)	TCAT	TTGC
(AAV4_b1)	ATAA	GAAC
(AAV4_b2)	GAAC	GGGT
(AAV4_b3)	GGGT	CTTT
(AAV4_b4)	CTTT	CTAC
(AAV4_b5)	CTAC	AACT
(AAV4_b6)	AACT	AGAC
(AAV4_b7)	AGAC	TCAT
(AAV4_b8)	TCAT	TTGC
(AAV5_b1)	ATAA	GAAC
(AAV5_b2)	GAAC	GGGT
(AAV5_b3)	GGGT	CTTT
(AAV5_b4)	CTTT	CTAC
(AAV5_b5)	CTAC	AACT
(AAV5_b6)	AACT	AGAC
(AAV5_b7)	AGAC	TCAT
(AAV5_b8)	TCAT	TTGC
(AAV6_b1)	ATAA	GAAC
(AAV6_b2)	GAAC	GGGT
(AAV6_b3)	GGGT	CTTT
(AAV6_b4)	CTTT	CTAC
(AAV6_b5)	CTAC	AACT
(AAV6_b6)	AACT	AGAC
(AAV6_b7)	AGAC	TCAT
(AAV6_b8)	TCAT	TTGC
(AAV8_b1)	ATAA	GAAC
(AAV8_b2)	GAAC	GGGT
(AAV8_b3)	GGGT	CTTT
(AAV8_b4)	CTTT	CTAC
(AAV8_b5)	CTAC	AACT
(AAV8_b6)	AACT	AGAC
(AAV8_b7)	AGAC	TCAT
(AAV8_b8)	TCAT	TTGC
(AAV9_b1)	ATAA	GAAC
(AAV9_b2)	GAAC	GGGT
(AAV9_b3)	GGGT	CTTT
(AAV9_b4)	CTTT	CTAC
(AAV9_b5)	CTAC	AACT
(AAV9_b6)	AACT	AGAC
(AAV9_b7)	AGAC	TCAT
(AAV9_b8)	TCAT	TTGC